Geophysical Modeling of a Possible Blind Geothermal System Near Battle Mountain, NV

[1]Tait Earney, [1]Jonathan Glen, [1]Jared Peacock, [2]James Faulds, [1]William Schermerhorn, [1]Grant Rea-Downing, [1]Jacob Anderson, [2]Cary Lindsey, [2]Maria Richards

[1]U.S. Geological Survey, Moffett Field, CA 94035

[2]University of Nevada, Reno, Great Basin Center for Geothermal Energy, Nevada Bureau of Mines and Geology, Reno, NV 89557

Keywords

Geothermal, hydrothermal systems, geophysics, gravity, magnetic, magnetotelluric, 2D modeling, 3D modeling, Argenta Rise, Basin and Range, Nevada

ABSTRACT

The northeastern portion of the Reese River basin in north-central Nevada is the focus of detailed geophysical and geological studies as part of the INGENIOUS project, which aims to identify new, commercially viable hidden geothermal systems in the Great Basin region of the western U.S. This location, herein referred to as Argenta Rise, occupies a broad (~15km wide) left-step between major range-front fault systems along the northwestern edge of the Shoshone Range and Argenta Rim, with numerous ENE-striking intra-basin faults presumably accommodating sinistral-normal oblique slip across the step-over. Four discrete regions have been identified within the study area that have favorable structural settings for hosting a blind hydrothermal system. However, with no definitive or extensive surface manifestations of an active hydrothermal system (e.g., geysers, steam vents, sinter, etc.), detailed geophysical studies are necessary to resolve subsurface geology and structure, and identify zones of enhanced structural complexity that may promote hydrothermal fluid flow. Hence, we collected high-resolution gravity, MT, and rock property data (density, magnetic susceptibility), and analyzed the recently acquired GeoDAWN aeromagnetic data to characterize potential geothermal resources in this region. Using the new geophysical datasets, we jointly modeled gravity and magnetic data along a series of intersecting 2D profiles that integrated information from recent, local-scale fault mapping. Rock property measurements performed on outcrops and hand samples throughout the study area constrained the models. The MT data were used to construct a 3D resistivity model that highlights the location of inferred alteration and fluids in the subsurface. Combined MT and potential field results reveal which structures may be most important for controlling hydrothermal fluid migration, as well as which geologic units may host hydrothermal fluids. Our gravity derived depth to basement surface

coincides well with the base of shallow conductive anomalies, suggesting hydrothermal fluids may be confined to basin fill sediments and volcanics. This work supports our development of 3D geophysical and geologic models that are focused along the western flank of the northern Shoshone Range and aids the process of selecting sites for temperature gradient drilling.

1. Introduction

The northeastern Reese River basin was initially identified for having high geothermal resource potential in the Nevada Play Fairway Analysis (PFA; DeAngelo, 2019; Faulds et al., 2019). Subsequently, this area was chosen for detailed geological and geophysical investigations as part of the Innovative Geothermal Exploration through Novel Investigations Of Undiscovered Systems (INGENIOUS) project (Ayling et al., 2022; Earney et al., 2022; Williams et al., 2022; Earney et al., 2023). Argenta Rise is located approximately 15 km southeast of Battle Mountain, NV, along the western flank of the northern Shoshone Range within the north-central Basin and Range Province (Figure 1). The Beowawe Geysers, an active geothermal area with numerous geysers and sinter deposits is ~15 km further east of Argenta Rise at the southern end of Whirlwind Valley. The Beowawe flash powerplant was established in 1985, and produced 16.7 MW from a roughly 200°C resource (Benoit and Stock, 1993). Although the geothermal resource at this location has degraded over time (Benoit and Stock, 1993), presumably due to recharge of cold meteoric water, the powerplant generated 13.7 MW of electricity in 2018 (Ayling, 2020). Argenta Rise lacks definitive surface manifestations of active thermal features, such as those observed at the Beowawe Geysers; however, it occupies a favorable structural setting thought to be conducive to hydrothermal up-flow (Faulds et al., 2011; Faulds and Hinz, 2015; Faulds et al., 2024). Faulds et al. (2024) identified two discrete regions with potentially elevated shallow temperatures proximal to the range-front fault zone on the western side of the northern Shoshone Range (Figure 1, inset map). To further refine areas favorable for geothermal activity at Argenta Rise, we conducted high-resolution gravity, magnetotelluric (MT), and physical property surveys, and analyzed Geoscience Data Acquisition for Western Nevada (GeoDAWN; Glen and Earney, 2023, 2024) aeromagnetic data to map and model subsurface geology and structure. Model parameters are constrained by physical property measurements (density, magnetic susceptibility) collected from hand samples and outcrops of the relevant geologic units throughout the northern Reese River basin and adjacent ranges. Our results support ongoing efforts to develop three-dimensional (3D) geologic and structural models, and identify specific sites for temperature gradient drilling.

2. Geologic Framework

Argenta Rise occupies a nearly 15 km wide left-step between major ENE-trending range-front fault systems along the northwestern edge of the Shoshone Range and at Argenta Rim (Figure 1). Numerous ENE-striking intra-basin faults presumably accommodate sinistral-normal oblique slip across the step-over. Beyond the favorable structural setting, there are two large-scale crustal features that make this region particularly favorable for geothermal resource investigations: 1) the Northern Nevada Rift (NNR); and 2) regionally high background conductive heat flow (Figure 1, index map). The NNR is a series of several narrow, arcuate, NNW-trending features that extend for at least 500 km from southern Nevada to the Nevada-Oregon border (McKee and Noble, 1986; Blakely and Jachens, 1991). The eastern segment of the NNR (Stewart et al., 1975; Zoback, 1979; Glen and Ponce, 2002) passes just east of the study area. Studies have proposed that the NNR was caused by a highly magnetic, mafic dike swarm that intruded the upper crust through deep-seated

crustal fractures that were reactivated in the middle Miocene during the passing of the Yellowstone hotspot along the Oregon-Idaho border (Zoback and Thompson, 1978; Glen and Ponce, 2002). The stresses induced by magma emplacement, and the contrast in physical properties between NNR-related intrusions and the surrounding country rock likely make the boundaries of the NNR structurally weak, and prone to faulting and fracturing. In regions with high strain rates, such as the Basin and Range (Zeng, 2022), these structures can frequently be reactivated, maintaining permeable pathways for deep circulating hydrothermal fluids. Thus, characterizing faults and fractures associated with the NNR will play an important role in understanding and identifying potential geothermal resources at Argenta Rise. This area also has anomalously high background conductive heat flow, largely as a result of regional extension within the Basin and Range. The study area sits on the eastern edge of the Battle Mountain High, a lobe of high heat flow in north-central Nevada with average surface heat flow estimates of 100+ mW/m^2 (Sass et al., 1971). Based on new maps of conductive heat flow within the Basin and Range (DeAngelo et al., 2022), estimated surface heat flow values at Argenta Rise are ~97.6 mW/m^2, and across the entire Basin and Range heat flow values are on average ~78.6 mW/m^2. These data suggest, at least regionally, that there is a higher potential of encountering geothermal resources at economically feasible depths in the north-central Basin and Range.

At Argenta Rise, the stratigraphy pertinent to our modeling efforts consists of highly deformed and thrusted Paleozoic siliciclastic and carbonate rocks that are overlain by minor deposits of Mesozoic sediments and intruded by Mesozoic and Tertiary granitoids (Crafford, 2007). Overlying these units are locally voluminous packages of Cenozoic volcanics and basin fill sediments (Crafford, 2007). The Paleozoic units, exposed along the northern Shoshone Range, at Battle Mountain, and in small outcrops at the southern end of the Sheep Creek Range, are presumed to be the primary basement lithologies throughout the northern Reese River basin. Although discrete intrusive bodies (i.e., dikes) related to the NNR are mapped at the surface in the northern Shoshone Range (Ramelli et al., 2001; John and Wrucke, 2003; Ramelli et al., 2017), the bulk of these rocks occur at depth along a NNW-trend through the northern Shoshone Range and Sheep Creek Range on the east side of the study area (Watt et al., 2007). For the purposes of two-dimensional (2D) and 3D modeling in this project, we generalize the Nevada state geological map (Crafford, 2007) within the region surrounding the study area by grouping together units that would be expected to have similar physical properties (density, magnetic susceptibility, magnetic remanence; Figure 1).

The two predominant fault orientations observed at Argenta Rise trend NNW and ENE, recording the transition from NNR-related ENE-WSW directed extension in the middle Miocene to the NW-SE directed extension characteristic of the modern-day Basin and Range, respectively (Zoback et al., 1994). Complex interactions between these opposing fault sets create numerous structurally favorable zones for promoting hydrothermal fluid flow within the study area (Faulds et al., 2011; Williams et al., 2022; Faulds et al., 2024). The geophysical data presented herein delineate concealed intra-basinal faults, and resolve subsurface fault interactions, providing a more complete view of subsurface fault complexity.

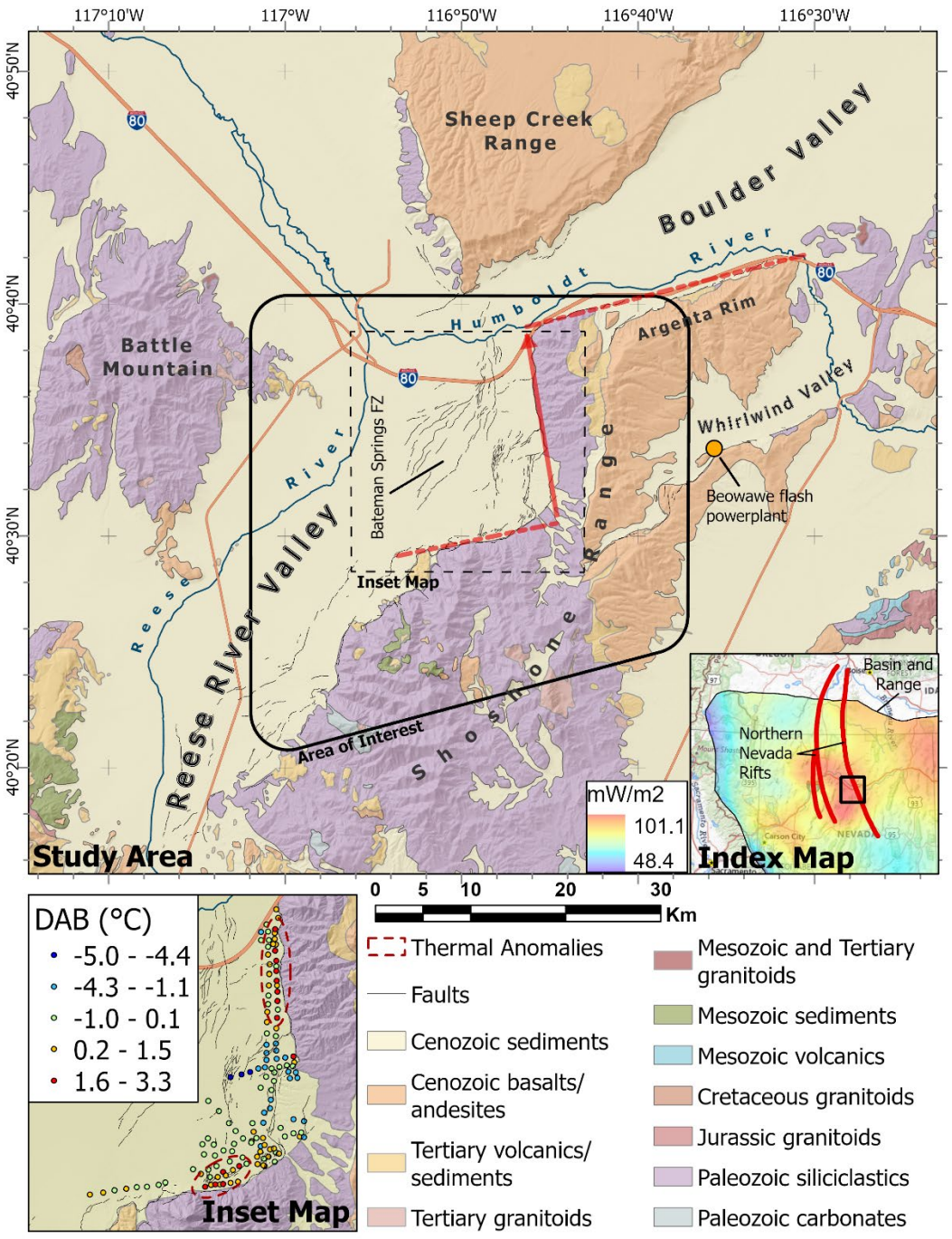

Figure 1: Study Area – Digital elevation model (DEM) hillshade (U.S Geological Survey, 2021a) overlain by simplified geologic map (adapted from Crafford, 2007). Faults are a compilation of existing (USGS, 2021a), and newly identified faults mapped by the University of Nevada, Reno (UNR) using lidar (U.S. Geological Survey, 2021b). The dashed red lines and red arrow indicate the left-step between range-front fault zones along the northwestern edge of the Shoshone Range (southern dashed red line) and Argenta Rim (northern dashed red line). Inset Map – 2-meter temperature survey conducted by UNR in July and November 2021 measured in degrees above background (DAB; Faulds et al., 2024). Index Map – Regional location map showing the location of the study area, the boundary of the Basin and Range, traces of the NNR (Glen and Ponce, 2002), and background conductive heat flow (DeAngelo et al., 2023).

3. Geophysical Data

Geophysical methods are valuable tools for investigating geothermal systems because they facilitate mapping of subsurface structures which may inhibit or host fluid flow and can be used to help resolve basin depths and geometries. Natural variations in gravity, magnetic, and electrical fields arise due to lateral and vertical contrasts in physical properties (e.g., density, magnetic susceptibility/remanence, and conductivity, respectively), which can reflect facies changes, presence of hydrothermal fluids, alteration products of hydrothermal fluids, offset across faults, and/or geological contacts. At Argenta Rise, the geology is quite varied, consisting of mafic igneous rocks, siliciclastic and carbonate rocks, granitoid intrusives, and tuffaceous and sedimentary rocks. The strong contrast in physical properties between these geologic units leads to distinct gravity, magnetic, and conductivity anomalies. We present new gravity, magnetic, and magnetotelluric data collected across the northern Reese River basin. We use various derivative, filtering, and modeling methods to characterize concealed geology and structures.

3.1 Gravity

A total of 1,207 new gravity measurements were collected in 2021 and 2022, encompassing ~2,000 km^2 of the northern Reese River basin and adjacent ranges. These data augmented an existing network of 3,899 gravity measurements from the surrounding region (Ponce, 1997; Hildenbrand et al., 2002 [PACES]; PACES database was made available from University of Texas, El Paso on 5/29/2018 [Ben Drenth, U.S. Geological Survey, written comm., March 2021]), improving regional coverage in areas of sparse control and providing detailed coverage (200 to 300 m station spacing) across range front and intra-basin structures. Isostatic anomaly values were calculated using standard gravity reduction methods (Blakely, 1995), assuming an average crustal density of 2,670 kg/m^3, a density contrast of 400 kg/m^3 at the crust-mantle boundary, and a sea level crustal thickness of 25 km. The isostatic anomalies were gridded using a minimum curvature routine with a cell size of 400 m. A residual isostatic anomaly map was subsequently generated (Figure 2) to facilitate structural mapping and interpretation of subtle anomalies produced by shallow crustal features that might otherwise be difficult to recognize in the presence of regional fields.

3.2 Magnetics

Magnetic data reveal subtle fluctuations in the magnetic field that reflect variations in the magnetization of rocks in the subsurface, and are particularly useful in regions where bedrock may be concealed by young basin fill sediments. In the northern Reese River basin, the strong contrast in magnetic properties (magnetic susceptibility and remanent magnetization) between the predominant lithologies (young sedimentary deposits [low magnetic properties], Cenozoic volcanics [high magnetic properties], and Paleozoic basement rocks [low magnetic properties]) results in distinct magnetic anomalies. These anomalies delineate structures such as faults and contacts that may provide natural permeable pathways for hydrothermal fluids.

The recently acquired GeoDAWN survey included a high-resolution aeromagnetic survey over northern and western Nevada and eastern California (Glen and Earney, 2024), and spans our study area at Argenta Rise. The survey was flown with a nominal flight height of 150 m above terrain over areas with low topographic relief and 200 m above terrain over mountain ranges. Flight lines were flown along an azimuth of 90 degrees and spaced 400 m apart, while tie lines were flown along an azimuth of 180 degrees and spaced 4,000 m apart. Magnetic data were recorded at 10 Hz.

The total field (TF) magnetic anomaly was gridded using a cell size of 100 m. We applied a number of derivative and filtering methods to this grid to simplify anomalies and aid interpretations of structural features. The reduced-to-pole (RTP) transformation (Blakely, 1995) was applied to the TF magnetic anomaly map to effectively center magnetic anomalies over their sources (Figure 3A). Additionally, several residual grids were created to highlight very subtle, shallow anomalies associated with young intra-basinal Quaternary faults (Figure 3B). To produce the residual grids, we upward continued the TF map a distance of 50 m and subtracted the result from the original TF map, then recalculated the RTP anomaly.

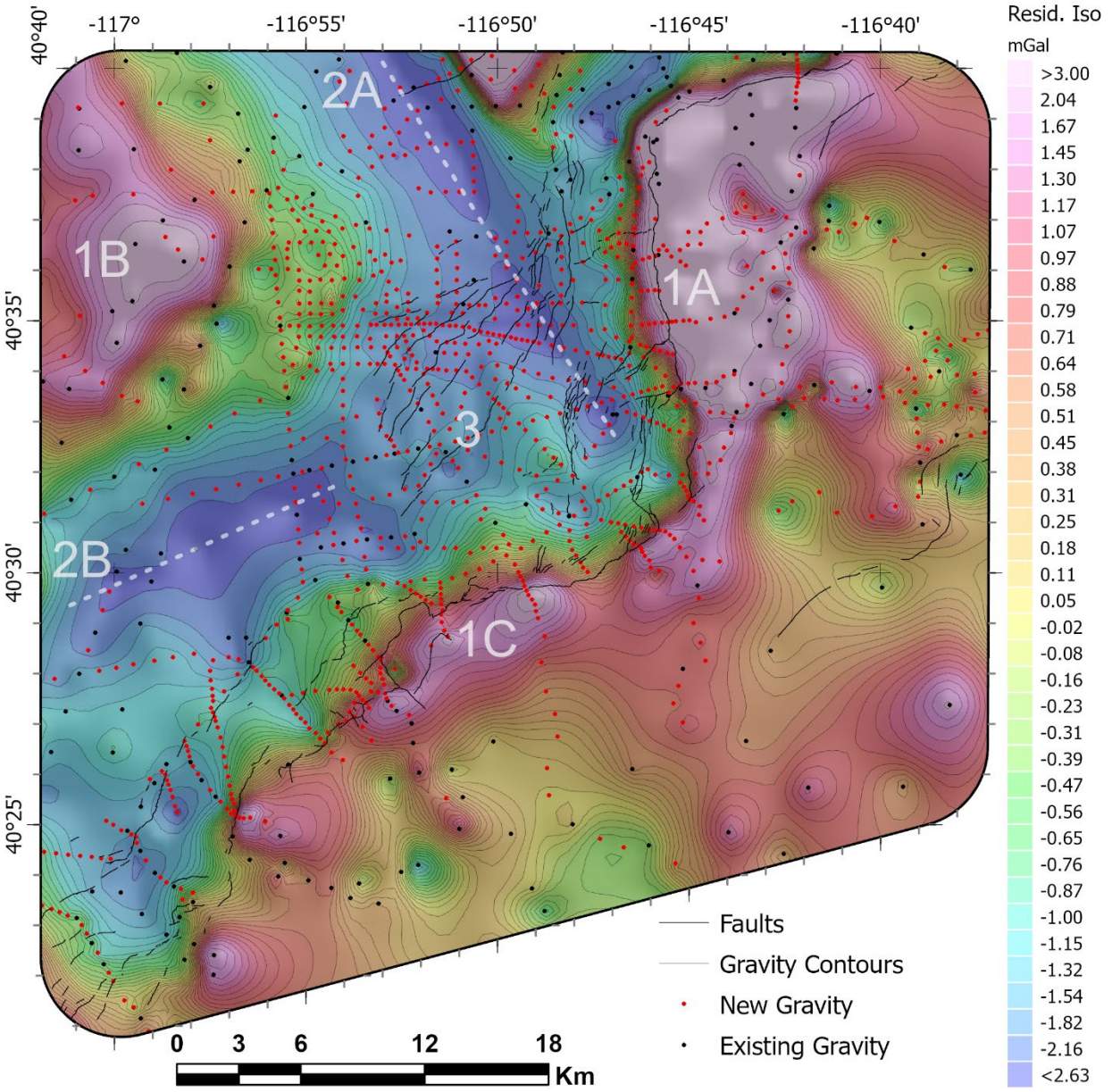

Figure 2: Residual isostatic anomaly map overlain by faults (dark black lines), gravity contours (light black lines; contour interval corresponds to bins in the 'Resid Iso' color bar), new gravity stations (red dots), and existing gravity stations. Labeled features are described in the Discussion section of this manuscript.

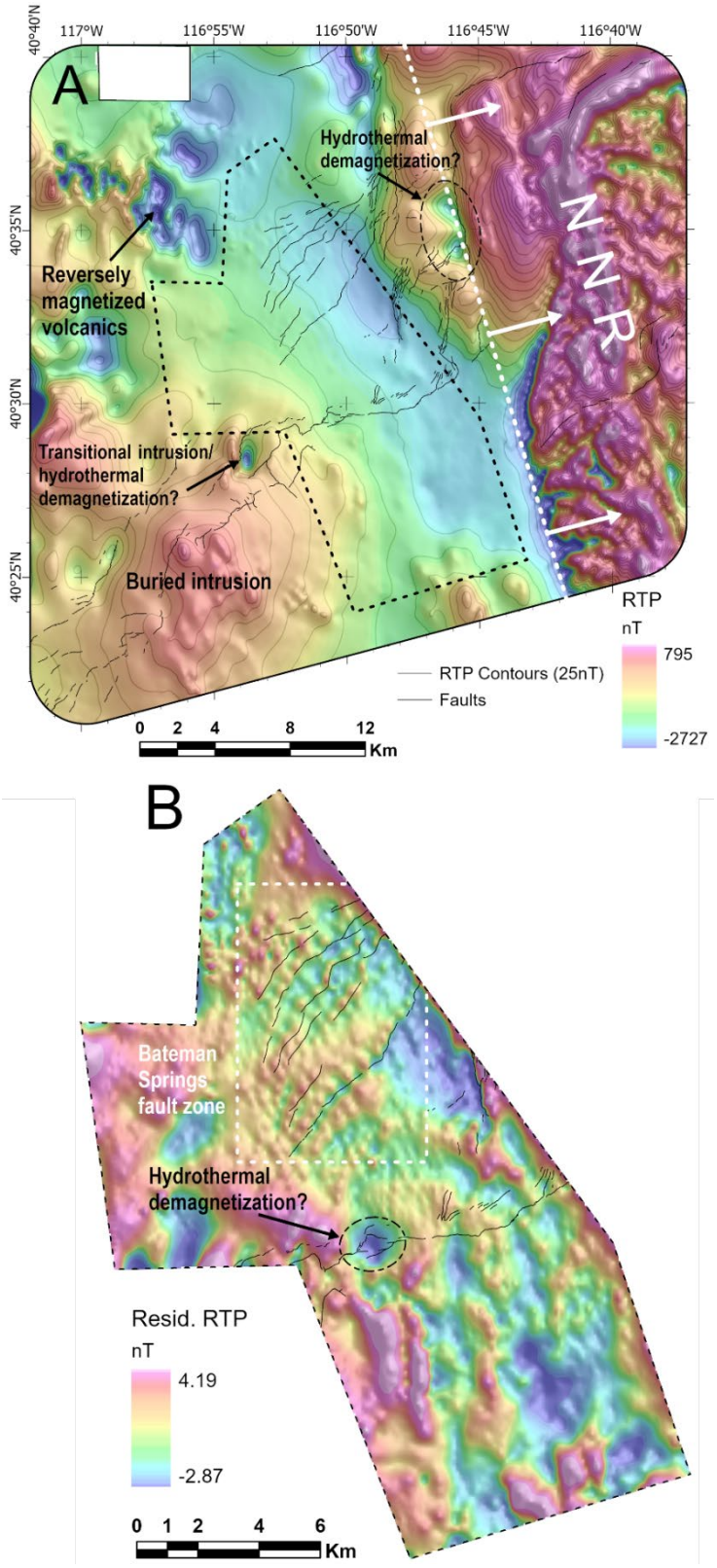

Figure 3: RTP magnetic anomaly (A), and residual RTP magnetic anomaly (B) overlain by faults (black lines). Dashed black line on panel A indicates the extent of the grid in panel B. Features pertinent to this study are labeled and described in the Discussion section of this manuscript.

3.3 Magnetotellurics

Magnetotellurics (MT) is a passive electromagnetic geophysical method that can be used to infer subsurface electrical conductivity structure by measuring the Earth's electrical response to natural time-varying magnetic fields. The MT method is particularly well suited for geothermal studies as it can facilitate imaging of subsurface clay caps, zones of hydrothermal alteration, heat sources, hydrothermal fluids, and thermally enhanced zones (Newman et al., 2008; Munoz, 2014).

In May 2022, MT data were collected at 43 locations spanning an area of ~200 km^2 across the core of the study area. Magnetic fields were measured with Zonge International Inc. ANT4 induction coils (Tucson, AZ). Electric fields were measured with Borin Stelth 1 Ag-AgCl electrodes (Culver City, CA) placed in saturated bentonite clay bags for better contact resistance. Both the magnetic and electric fields were recorded with ZEN data loggers developed by Zonge International Inc. (Tucson, AZ). The instruments were left recording for about 24 hours, providing reliable resolution of the subsurface conductivity structure for the upper two to three kilometers of the Earth's crust. MT data were used to generate a 3D electrical conductivity model of the subsurface using ModEM (Kelbert et al., 2014). From the 3D model, we extracted 2D plan maps at pre-determined depths (relative to sea level) to highlight conductive anomalies at various depths of investigation that might indicate the locations of hydrothermal fluids or their alteration products (Figure 4). Additionally, we extracted 2D cross sections from the 3D model along our 2D geophysical profiles to facilitate the interpretation of which structures may host hydrothermal fluid flow in the shallow subsurface.

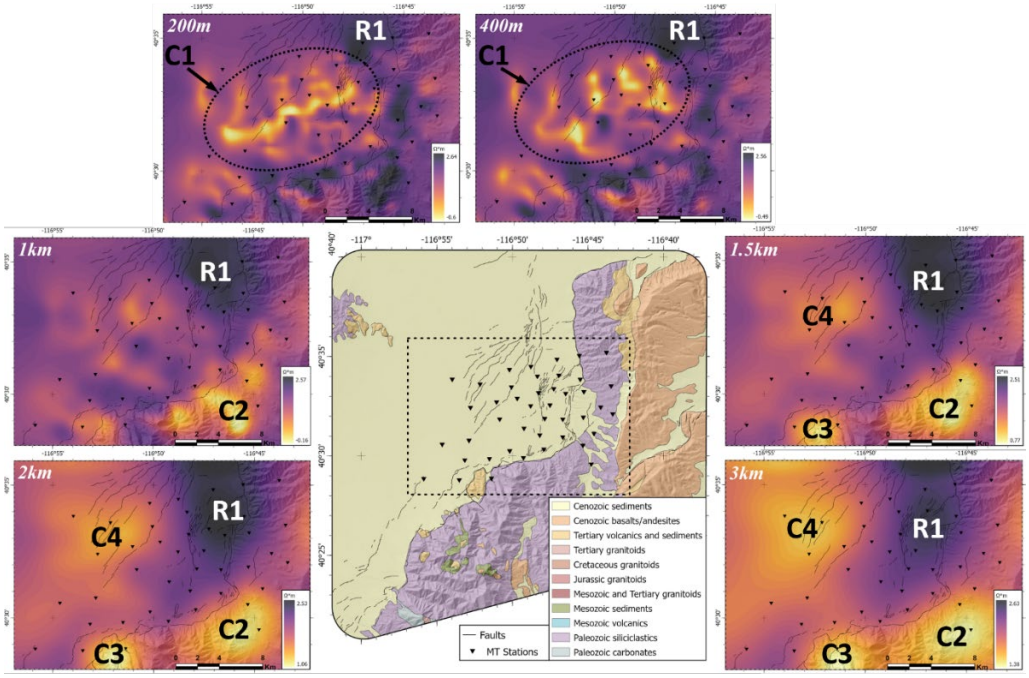

Figure 4: Depth slices through 3D conductivity model. (Center) DEM (U.S. Geological Survey, 2021) hillshade overlain by the generalized geologic map, faults (black lines) and MT stations (inverted black triangles). The dashed black rectangle indicates the extent of the depth slices. These images highlight the conductivity structure at depths of 200 m (upper left), 400 m (upper right), 1 km (mid left), 1.5 km (mid right), 2 km (lower left), and 3 km (lower right) beneath Argenta Rise. Conductive and resistive anomalies (i.e., C1-4, R1, respectively) are described in the Discussion section of this manuscript.

4. Structural Mapping

We performed a horizontal gradient analysis of the gravity and magnetic grids to detect abrupt lateral changes in density and magnetization, and thereby elucidate subsurface structural patterns. Subsurface structures typically manifest as steep gradients in potential field data, and can be mapped by analyzing horizontal gradient maxima (HGM; Grauch and Cordell, 1987; Cordell and McCafferty, 1989; Blakely and Simpson, 1986), which tend to lie over sub-vertical structures. For the TF magnetic data, we first calculated the pseudogravity (Blakely, 1995). The pseudogravity transformation effectively centers TF magnetic anomalies over their respective source bodies, and simplifies their interpretation. We then calculate horizontal gradient maps of the gravity and pseudogravity grids, and following Phillips et al. (2007), calculate HGM using a routine that identifies laterally continuous ridges in horizontal gradient maps. Discrete maxima were then connected into continuous lines (or lineations) based on user specified distance and azimuth tolerance relationships to adjacent maxima (Athens, 2018; Figure 5).

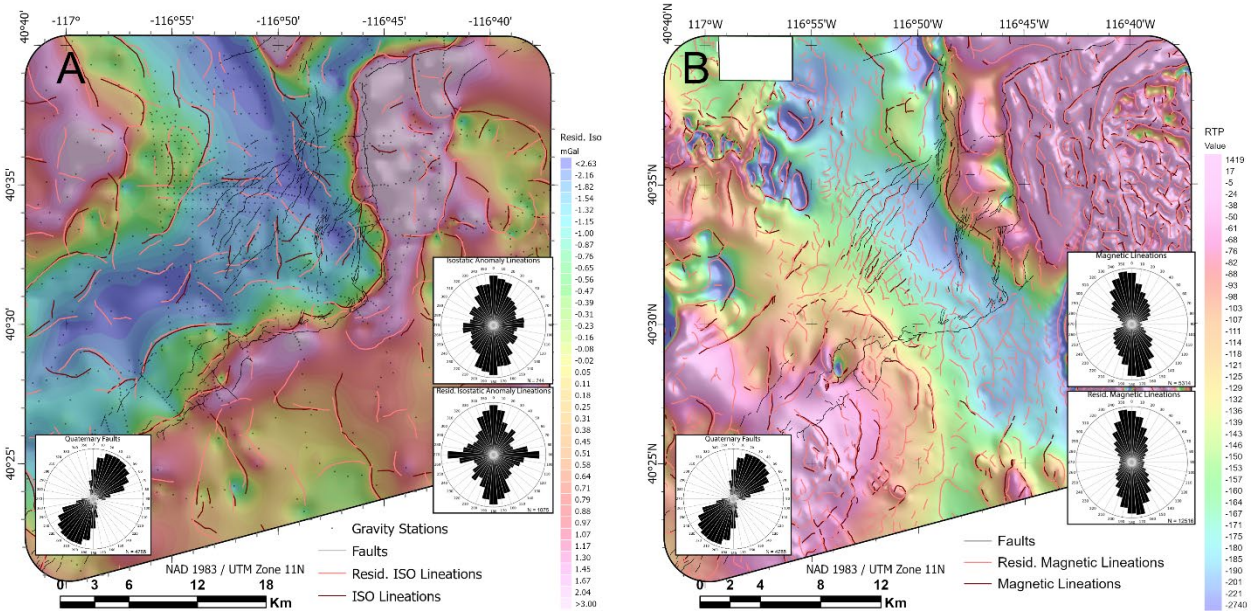

Figure 5: A) Residual isostatic anomaly overlain by gravity stations (black dots), faults (black lines), and lineations derived from the isostatic and residual isostatic anomalies (dark red and light red lines, respectively. Rose diagrams show trends of Quaternary faults (lower left), lineations derived from the isostatic anomaly (upper right) and lineations derived from the residual isostatic anomaly (lower right). B) RTP magnetic anomaly overlain by faults (black lines) and lineations derived from the magnetic and residual magnetic anomalies (dark red and light red lines, respectively). Rose diagrams show trends of Quaternary faults (lower left), lineations derived from the pseudogravity anomaly (upper right), and lineations derived from the residual pseudogravity anomaly (lower right).

5. Geophysical Modeling

To characterize subsurface stratigraphy and structure we constructed 2D and 3D potential field models utilizing both forward and inverse methods. Physical property measurements (density, magnetic susceptibility, magnetic remanence) from hand samples and outcrops of relevant geologic units throughout the region informed model parameters. All models are consistent with the mapped surface geology represented in the generalized geological map.

5.1 Depth to Basement

We perform a 3D inversion of gravity anomalies, using methods described by Jachens and Moring (1990), to estimate the geometry of the pre-Cenozoic basement surface beneath the northern Reese River basin (Figure 6). This method is an iterative procedure that combines gravity data, surface geology, and an estimate of the density of Cenozoic deposits to approximate the thickness of young basin fill. We separated the isostatic anomaly into two components: 1) a basement gravity field (representing crystalline, pre-Cenozoic, and intrusive rocks); and 2) a basin fill gravity field (representing overlying Cenozoic basin fill deposits). We simplify the surface geology of the Nevada state geologic map (Crafford, 2007), and reclassify all units into two categories: basement (generally any crystalline, pre-Cenozoic, or intrusive rocks) and Cenozoic deposits. For the purposes of this project, we reclassify all Cenozoic volcanics as Cenozoic sediments being that there are no volcanic units that are both thick enough (greater than several hundred meters) and dense enough to appreciably affect the regional gravity field in the study area. During the inversion the basement density is allowed to vary laterally while a vertical density gradient function (Jachens et al., 1996) is enforced in the basin fill deposits (see 'Quaternary Sediments', Table 1). To constrain the inversion solutions, we incorporate publicly available well data from three sources: oil and gas (Nevada Bureau of Mines and Geology, 2023b), geothermal (Nevada Bureau of Mines and Geology, 2023a), and water wells (Nevada Division of Water Resources, 2023).

This style of depth to basement estimate contains a substantial amount of uncertainty and is often only accurate to within 20% of the total basin depth in areas without well constraints (Jachens et al., 1996). Ambiguity in the gravity method, local density-depth variations in overlying basin fill deposits, and the assumption that basin fill density varies in the vertical direction only will often lead to an underestimation of true basin depth. Furthermore, basement lithologies, while modeled as a single unit in the inversion, are highly variable and heterogeneous throughout the study area, representing a wide range of densities. Nonetheless, our inversion results provide a qualitative characterization of relative variations in the basement surface. We use that characterization to guide regional interpretations of basin geometry and inform the development of our 2D and 3D geophysical models.

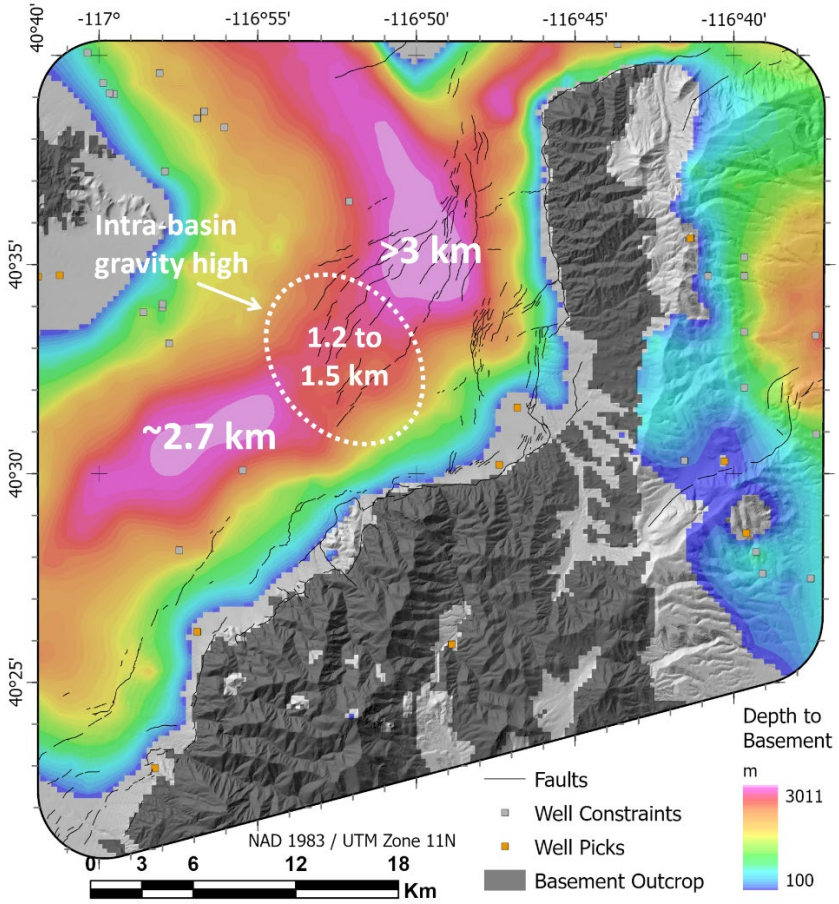

Figure 6: DEM (U.S. Geological Survey, 2021) hillshade overlain by depth to pre-Cenozoic basement map, faults (black lines), minimum constraint wells (i.e., wells not intercepting the basement; grey squares), basement intercepting wells (orange squares), and locations of basement outcrop (dark grey areas). Light grey areas are locations where basement is interpreted to be <100 m below the surface.

5.2 2D Modeling

A series of 12, 2D joint gravity and magnetic potential field models were created along profiles spanning the northern Reese River basin (Figure 7). Six of these profiles (WV1, WV2, WV3, WV4, WV5 and NNRA) were adapted from Watt et al., (2007) and updated to be consistent with the modeling goals of this study. Although geophysical models are typically placed orthogonal to the primary structural trend that is being characterized, we also consider the underlying gravity data density and attempt to focus on regions with dense data coverage that still captures key features and structures that may be important for controlling hydrothermal activity. Profile data are extracted from the gravity (isostatic anomaly) and magnetic (total field anomaly) grids with a sampling interval of 100 m along the profiles. Model bodies are assigned densities and magnetic susceptibility and remanence values based on physical property measurements when available (Table 1). Model body geometries are made to be consistent with the generalized surface geology. A total of 31 geologic units are modeled, representing 23 generalized 2D model layers with differing densities based on depth, and different remanent magnetizations. The model bodies are adjusted iteratively using a process of forward and inverse methods to reproduce the observed potential field anomalies within the limits imposed by the physical property data and surface geology (Figure 8).

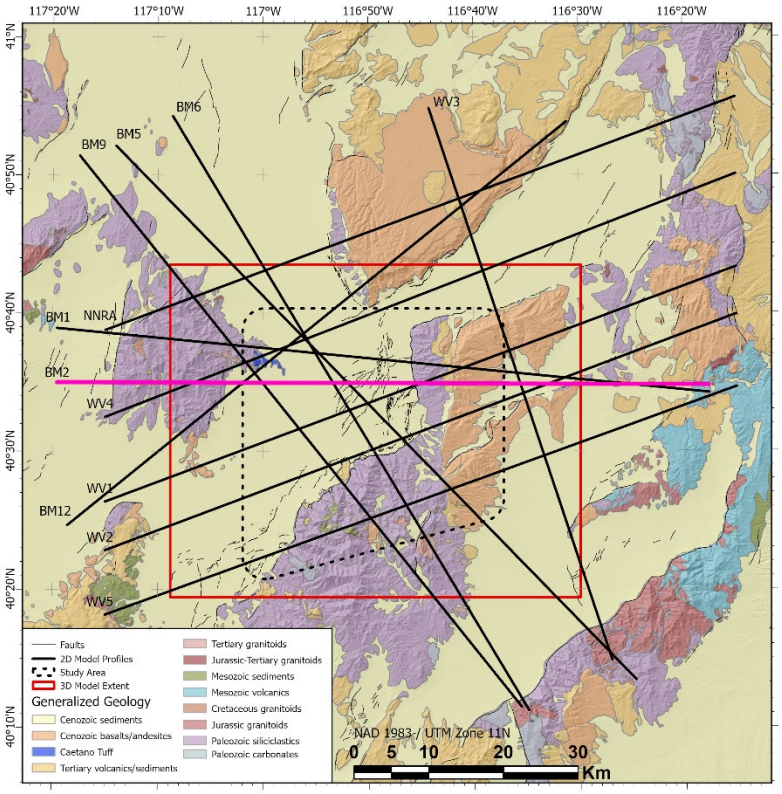

Figure 7: DEM (U.S. Geological Survey, 2021) hillshade overlain by generalized geologic map, faults (thin black lines), 2D model profile locations (thick black lines), the Argenta Rise study area (dashed black polygon), and the 3D model extent (red polygon; Figure 9). The 2D model profile indicated by the thick pink line (BM2) is presented herein (Figure 8).

Table 1: Physical property values used in 2D and 3D modeling. Physical properties include density (measured in kilograms/meter^3), magnetic susceptibility (Susc.; unitless, values reported in 10^{-3} SI), magnetic remanence (Rem.; measured in Ampere/meter), inclination (Inc.; measured in degrees), and declination (Dec.; measured in degrees). Values determined by measurements performed on hand samples and outcrops for this project.

Unit	Description	Density kg/m^3	Susc. (x10^{-3}) SI	Rem. A/m	Inc. degrees	Dec. degrees
QTs	Quaternary sediments: 0 – 200 m	2,020	*	*	*	*
	Quaternary sediments: 200 – 600 m	2,120	*	*	*	*
	Quaternary sediments: 600 – 1200 m	2,320	*	*	*	*
	Quaternary sediments: >1200 m	2,420	*	*	*	*
QTba	Quaternary - Tertiary basalts/andesites	2,550	0.025	1	64	12.5
Caetano	Tertiary Caetano Tuff	2,120	0.005	1.9	-66.5	156.3
Tvs	Tertiary volcanics/sediments	2,400	0.013	*	*	*
Ti	Tertiary granitoids	2,670 – 2,720	0.007 – 0.013	*	*	*
Ki	Cretaceous granitoids	2,670 – 2,720	0.008 – 0.013	*	*	*
Ji	Jurassic granitoids	2,670 – 2,750	0.006 – 0.013	*	*	*
TKJi	Mesozoic and Tertiary granitoids	2,670 – 2,750	0.035	*	*	*
Ms	Mesozoic sediments	2,600	*	*	*	*
Mv	Mesozoic volcanics	2,600	0.010	*	*	*
Pzu	Paleozoic siliciclastics	2,660	0.001	*	*	*
Pzc	Paleozoic carbonates	2,700	*	*	*	*
NNR2	NNR (lightly intruded basement)	2,670 – 2,770	0.005 – 0.025	0.5	64	12.5
NNR1	NNR (heavily intruded basement)	2,700 – 2,800	0.031 – 0.038	1	64	12.5

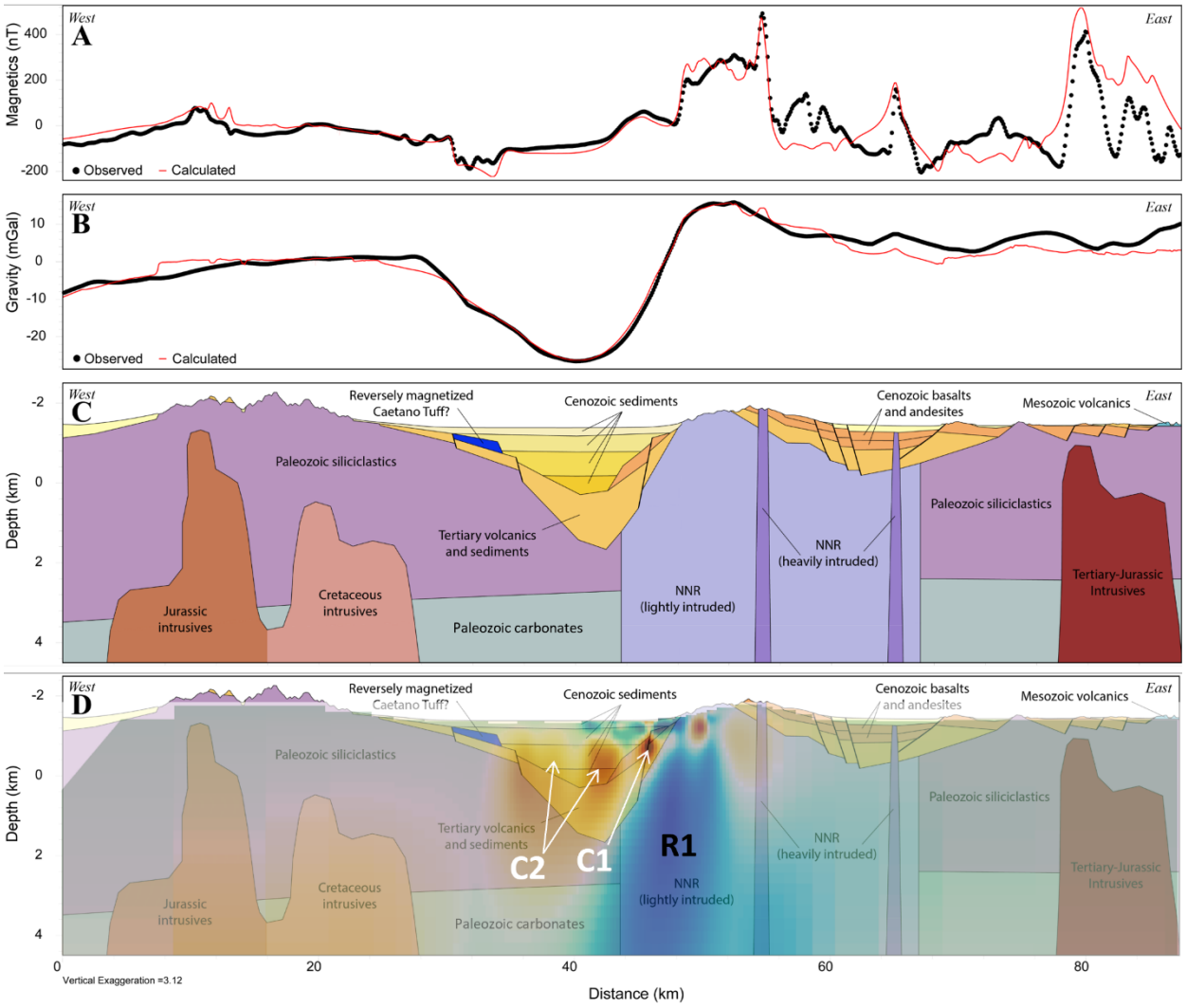

Figure 8: Joint gravity and magnetic potential field model along profile BM2 (profile location indicated by pink line on Figure 7). Magnetic data (panel A) are extracted from the total field anomaly and gravity data (panel B) are extracted from the isostatic anomaly. Observed anomalies are indicated by the black dots, and the calculated model responses are indicated by the red lines. Model bodies (panel C) are assigned densities and magnetic susceptibility and remanence values based on physical property measurements performed on outcrops and hand samples collected in Reese River basin and surrounding ranges. Resistivity anomalies (panel D) overlain on model bodies highlight near surface conductors that could represent hydrothermal fluids and/or zones of alteration along faults and contacts. Conductive and resistive anomalies (i.e., C1, C2, and R1) are described in the Discussion section of this manuscript.

5.3 3D Modeling

A 3D joint gravity and magnetic potential field model is developed using the Oasis Montaj® GM-SYS 3D Modeling software extension (Seequent, 2023). The 23 generalized 2D model layers are further simplified to 10 layers for the 3D model and provide initial constraints. Surfaces in the 3D model are adjusted through structural inversions to minimize misfit between the observed and calculated anomalies (Figure 9). There are several ambiguities in the model area related to the depth and geometry of sources. One of the layers, representing young, reversely magnetized

volcanics, did not reproduce either the geometry, or magnitude of the magnetic low at the southeast corner of Battle Mountain (see 'Reversely magnetized volcanics' on Figure 9). We attribute this to the fact that this anomaly is relatively small, isolated, and not adequately represented in the 2D models. Therefore, we removed this layer from the 3D model, and instead created a voxel model over this anomaly and inverted on magnetic susceptibility, deriving a closed body isosurface, which when imported back into the 3D model, reproduces the magnetic low quite well. Another ambiguity pertains to the geometry and depth of the granitoids. Surficial outcrops of these units are relatively small, and we do not have an extensive inventory of physical property information on them. The density contrast between the granitoids and surrounding basement lithologies is presumed to be minor. However, some of the granitoids appear to have distinct magnetic anomalies associated with them. To model the granitoids in 3D, we performed a series of magnetic structural inversions on the granitoid layer, creating a tiered geometry in which the granitoids are more voluminous at depth, and more laterally restricted closer to the surface.

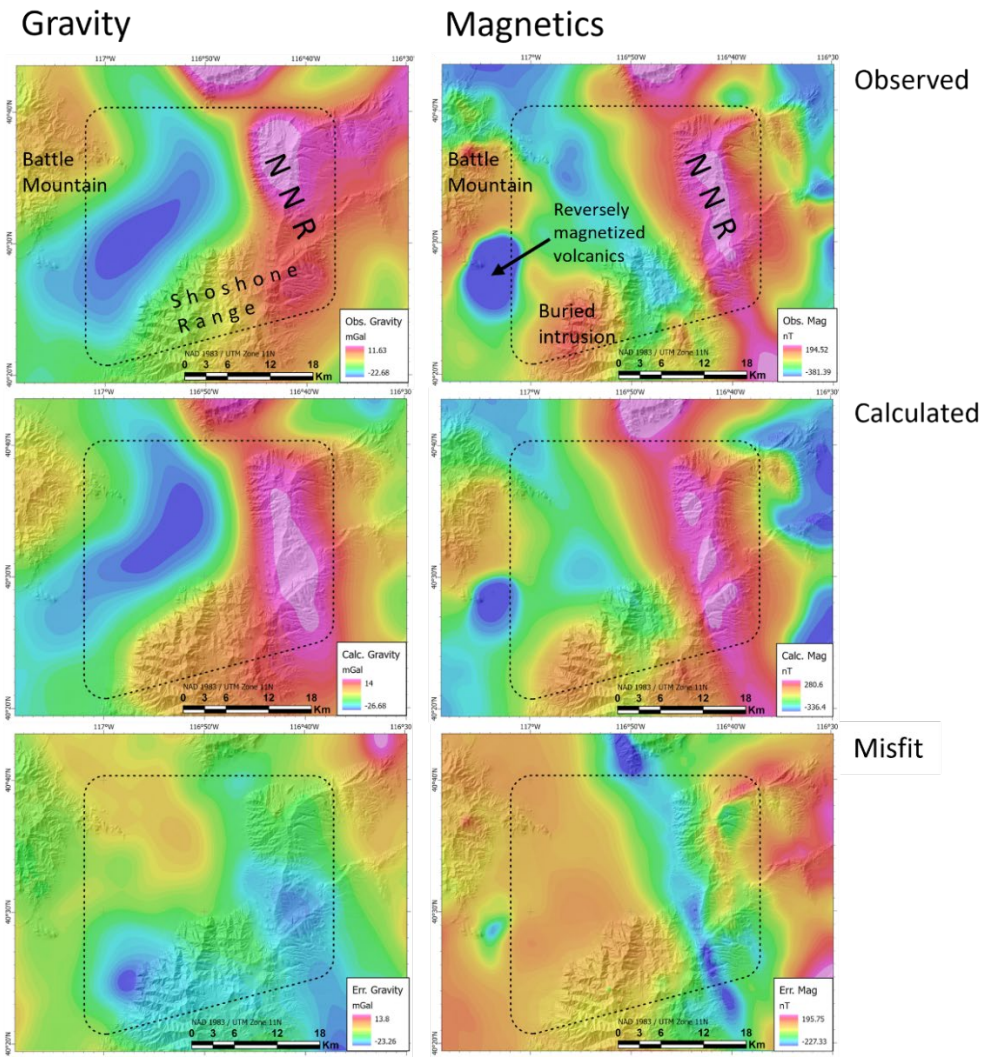

Figure 9: DEM (U.S Geological Survey, 2021) hillshade overlain by results of 3D joint gravity and magnetic potential field model showing observed gravity and magnetic anomalies (top), calculated model responses (middle), misfit between the observed and calculated anomalies (bottom). The Argenta Rise study area is indicated by the black dashed polygon. Model extent is indicated on Figure 7.

6. Discussion

The geophysical data and models presented here-in, reveal basin-bounding and concealed intra-basinal structures that may influence the development of a hydrothermal system at Argenta Rise. Anomalies observed in the gravity, magnetic and magnetotelluric datasets are used to constrain basin geometry and basin depth, delineate concealed contacts, faults, and fault extensions, and identify regions with subsurface fluid flow and/or hydrothermal alteration. Interpretations of these features are incorporated in the 2D and 3D models to provide a robust characterization of subsurface geology at Argenta Rise.

The gravity maps and depth-to-basement results constrain basin geometry and basin depth in the northern Reese River valley. The highs (areas 1A, 1B, and 1C on Figure 2) correspond to outcrops and near surface bodies of Paleozoic siliciclastic and carbonate rocks and middle Miocene NNR-related mafic intrusives, which tend to be relatively dense compared to other lithologies in the region. The two most prominent gravity lows (areas 2A and 2B on Figure 2) delineate two structurally controlled sub-basins beneath the northern Reese River basin; one trending NNW (area 2A) and the other trending ENE (area 2B). The NNW-trending sub-basin is asymmetric, with the trough of the gravity low displaced towards the east relative to the central axis of the basin between Battle Mountain and the northern Shoshone Range. The eastern edge of the gravity low has a distinct NNW-trend, which is notably different than the much more northerly trend of the current range-front fault zone bounding the western edge of the northern Shoshone Range. We interpret this gradient to represent the concealed, southeastward extension of the NNW-trending range-front fault zone bounding the west side of the southern Sheep Creek Range. Gravity values in this sub-basin gradually increase to the west, suggesting vertical deformation is primarily accommodated by the eastern range-front fault zones. The ENE-trending sub-basin is relatively more symmetric and truncated along its eastern extent by an approximately 10 km wide series of subtle intra-basin gravity highs (area 3 on Figure 2) that also delineate the west side of the southern portion of the NNW-trending sub-basin. The intra-basin gravity highs form a ridge-like feature across the Reese River basin and may be indicative of structural relief in the basement surface.

Our gravity derived depth-to-basement results (Figure 6) indicate maximum basin depths of >3 km in the southern portion of the NNW-trending sub-basin and ~2.7 km in the ENE-trending sub-basin. An intra-basin gravity high (area 3 on Figure 2; Figure 6) is situated between these two regions. Basin depths above the intra-basin gravity high are 1.2 to 1.5 km. If this feature is structurally controlled, it suggests that there could be 1.2 to 1.8 km of cumulative vertical displacement across the structures inferred along its periphery. The intra-basin gravity high could be a barrier to lateral flow of subsurface fluids between the NNW- and ENE-trending sub-basins or, alternatively the structural complexity may locally enhance permeability, promoting the vertical transport of fluids between the deep and shallow subsurface (Earney et al., 2018; Craig et al., 2021).

One of the most prominent features apparent in the GeoDAWN aeromagnetic data (Glen and Earney, 2023, 2024) is a NNW-trending region of magnetic highs in the eastern portion of the study area (labeled ‘NNR’ on Figure 3A). Numerous aforementioned studies (Stewart et al., 1975; Zoback and Thompson, 1978; Zoback, 1979; McKee and Noble, 1986; Blakely and Jachens, 1991; Glen and Ponce, 2002) have concluded that this feature is caused by a highly magnetic, mafic dike swarm that was emplaced in the middle Miocene. Large-scale crustal features, such as the NNR, typically have highly faulted and fractured boundaries which can serve as conduits for deep

circulating hydrothermal fluids. Numerous other features are interpreted from the aeromagnetic data, including shallowly buried, reversely magnetized volcanics (Figure 3A), buried intrusive bodies (Figure 3A), zones of possible demagnetization due to hydrothermal alteration (Figure 3A and 3B), and very subtle anomalies associated with young Quaternary faults along the Bateman Springs fault zone (Figure 3B). The residual magnetic lineations overall show a very strong northerly trend (Figure 5B). However, over the basin where magnetic gradients are much lower, there are numerous lineations with a distinct NNW-trend, a trend that is not well represented in Quaternary fault patterns within the study area. This trend is very similar to the trend of the NNR. Therefore, we interpret these features to represent relatively older structures that may relate to emplacement of the NNR. Many of the NNE-trending intra-basin faults associated with the Bateman Springs fault zone have subtle, but mappable anomalies associated with them (Figure 3B). Furthermore, the horizontal gradient analysis reveals that many of these faults extend further than they are currently mapped, in addition to identifying new structures that are currently unmapped. The recognition of these features and, more importantly, where these features intersect with northerly- and NNE-trending Quaternary faults may help identify additional areas with enhanced structural complexity that could support the development of a hydrothermal system.

Overall, the MT results (Figure 4) correlate well with the gravity derived depth-to-basement results (Figure 6) with nearly all of the conductors lying within the basin or slightly above the basement-basin fill contact (bottom panel on Figure 8 shows one example of this). As an exception, however, we note that strong conductors appear within basement lithologies at depth in the southern portion of the survey area (C2 and C3 on Figure 4). As there are currently no mapped hot springs in these areas, we interpret these anomalies as possible recharge zones, where meteoric fluids are entering the subsurface through a network of deep-seated fractures in the basement. Shallow and deep conductors (C1 and C4 on Figure 4, respectively) within the basin appear to line up nicely with the region of dispersed NE-striking faults associated with the Bateman Springs fault zone, and may represent the presence of saline groundwater or, alternatively, could be due to hydrothermal upwelling. A resistive body (R1 on Figure 4) is consistently present at all depths in the northeastern portion of the survey area, becoming more pronounced and expanding south and westward at deeper depths. This resistive body is interpreted to reflect the geometry of the basement surface at this location.

The 2D geophysical modeling we performed constrained the locations and relative amounts of offset along major faults and highlights which faults may be more conducive to hosting hydrothermal fluid flow. One of the primary advantages of 2D geophysical models is the ability to leverage high resolution geophysical data where available to make detailed structural interpretations that can be difficult to characterize in 3D. The 2D geophysical model presented here (Figure 8), has several correlations with the MT data that may indicate the presence of shallow hydrothermal activity. The strongest conductive anomaly (C1 on Figure 8) along the profile is co-located with a major, northerly-trending fault on the east side of the basin. The anomaly appears confined to a perched volcanic unit that overlies a package of mixed sedimentary and volcanic basin fill (Cenozoic basalts/andesites and Tertiary volcanics/sediments). However, the conductive anomaly does not appear to extend much deeper than the perched volcanic unit, suggesting that if this anomaly is due to the presence of hydrothermal fluids and/or alteration, the primary zone of upwelling may be occurring off-axis of this profile. Alternatively, this anomaly may reflect the presence of a shallow groundwater aquifer that is confined to the volcanics and localized around the fault due to an enhancement of permeability. The slightly less conductive, but more extensive

anomaly just to the west (C2 on Figure 8), correlates spatially with the Bateman Springs fault zone, and may indicate hydrothermal activity, or the presence of sediment-hosted meteoric groundwater. The large resistive body (R1 on Figure 8) is interpreted as NNR-intruded basement.

The 2D geophysical models provide discrete, detailed structural information about the subsurface. However, subsurface geology is inherently complex and difficult to characterize via 2D methods alone. The 3D geophysical model, presented here (Figure 9), provides a more robust means of testing the validity of our 2D models and, by extension, our conceptual model of the subsurface. Overall, the calculated gravity and magnetic responses of our 3D model layers agree quite well with the observed data as indicated by the relatively low error estimates. Inconsistencies within the 3D model are largely due to poor data distribution (primarily the sparse gravity data coverage in the south and southeastern portion of the Shoshone Range), and the complex, heterogeneous nature of the geology being modeled. Some of the misfit could be minimized by incorporating additional 2D model constraints. Nevertheless, the data from the 2D and 3D geophysical models provide insight regarding stratigraphic, structural and physical property relationships of subsurface geology at Argenta Rise.

7. Conclusions

We characterize the subsurface geology, constrain basin geometry, and map basin-bounding and concealed intra-basin structures at Argenta Rise using high-resolution geophysical data (i.e., newly collected gravity, MT, and physical property data and aeromagnetic data) to model geophysical anomalies and assist with identifying structural settings that are favorable to hydrothermal fluid flow. The gravity and depth-to-basement maps reveal two sub-basins beneath Argenta Rise with a potential structurally controlled, intra-basin high separating these two basins. Maximum basin depths are near 3 km. The horizontal gradient analysis of the aeromagnetic data suggests the presence of previously unmapped intra-basin structures (e.g., new faults and extensions of mapped faults), as well as extensions to mapped faults, and highlights subsurface structural complexity. When combined with the 2D geophysical models, the MT data indicate regions of potential hydrothermal activity, in some cases with strong conductive bodies co-located with faults and contacts. The 3D geophysical model shows that our conceptual model of basin geometry and structure (represented in the 2D geophysical models) is relatively accurate throughout the study area as indicated by the low error estimates. These data will support our planned development of a 3D geological model and aid the process of selecting sites for temperature gradient drilling.

Acknowledgements

This project is funded by U.S. Department of Energy – Geothermal Technologies Office under award DE-EE0009254 to the University of Nevada, Reno, and with support from the U.S. Geological Survey Energy Resources Program under the Geothermal Resource Investigation Project. Any use of trade, firm, or product names is for descriptive purposes only and does not imply endorsement by the U.S. Government. We thank Karen Christopherson, Randall Mackie, Stanley Mordensky, and Jacob DeAngelo for their thoughtful reviews of this manuscript.

REFERENCES

Athens, N. "Maxspots curvature." software available at: https://github.com/nathens/maxspots_curvature, (2018).

Ayling, B. "35 years of geothermal power generation in Nevada, USA: A review of field development, generation, and production histories." *Proceedings: 45th Workshop on Geothermal Reservoir Engineering*, Stanford University, Stanford, CA (2020), p. 12

Ayling, B., Faulds, J.E., Clark, A., Morales-Rivera, A., Sladek, C., Berti, C., Kreemer, C., Siler, D., Mlawsky, E., Gentry, E., Kleber, E., Burns, E., Warren, I., Batir, J., DeAngelo, J., Peacock, J., Witter, J., Queen, J., Glen, J.M.G., Kraal, K., Mann, M., Wagoner, N., Williams, N., Dobson, P., Micander, R., Koehler, R., Kirby, S., Brown, S., Earney, T.E., Cladouhos, T., Rickard, B., Trainor-Guitton, W., Lifton, Z. "INnovative Geothermal Exploration through Novel Investigations Of Undiscovered Systems (INGENIOUS) Project Introduction and Activity Update." *Proceedings: GRC Transactions*, 46, (2022).

Benoit, D., and Stock, D. "A case history at the Beowawe, Nevada geothermal reservoir." *Proceedings: GRC Transactions*, 17, (1993).

Blakely, R.J., and Simpson, R.W. "Approximating edges of source bodies from gravity or magnetic data." *Geophysics*, 51, (1986), doi: 10.1190/1.1442197.

Blakely, R.J., and Jachens, R.C. "Regional study of mineral resources in Nevada: Insights from three-dimensional analysis of gravity and magnetic anomalies." *Geological Society of America Bulletin*, 103, (1991).

Blakely, R. J. "Potential Theory in Gravity and Magnetic Applications." *New York, Cambridge University Press*, (1995).

Cordell, L., and McCafferty, A.E. "A terracing operator for physical property mapping with potential field data." *Geophysics*, 54, (1989), doi:10.1190/1.1442689.

Crafford, A.E.J. "Geologic map of Nevada." *U.S. Geological Survey Data Series*, 249, (2007).

Craig, J.W., Faulds, J.E., Hinz, N.H., Earney, T.E., Schermerhorn, W.D., Siler, D.L., Glen, J.M., Peacock, J., Coolbaugh, M.F., DeOreo, S.B. "Discovery and analysis of a blind geothermal system in southeastern Gabbs Valley, western Nevada, USA." *Geothermics*, 97, (2021).

DeAngelo, J. "Nevada geothermal favorability mapping, weights of evidence smoothed functions and refined methodology." *San Francisco State University*, masters thesis, (2019).

DeAngelo, J., Burns, E.R., Gentry, E., Batir, J.F., Lindsey, C.R., Mordensky, S.P. "Heat flow maps and supporting data for the Great Basin, USA." *U.S. Geological Survey Data Release*, (2022), doi: 10.5066/P9BZPVUC.

Earney, T.E., Schermerhorn, W.D., Glen, J.M.G., Peacock, J., Craig, J., Faulds, J., Hinz, N., Siler, D. "Geophysical investigations of a blind geothermal system in southern Gabbs Valley, Nevada." *Proceedings: GRC Transactions*, 42, (2018).

Earney, T.E., Glen, J.M.G., Ayling, B., Faulds, J., Siler, D., Dean, B., Zielinski, L.A., Schermerhorn, W.D., Williams, N., Wagoner, N., Morales-Rivera, A. "Characterizing structure and geology with potential field geophysics to assess geothermal resource potential near Battle Mountain, NV." *Proceedings: GRC Transactions*, 46, (2022).

Earney, T.E., Glen, J.M.G., Peacock, J., Faulds, J.E., Schermerhorn, W.D., Rea-Downing, G., Anderson, J.E. "Preliminary geophysical maps and models of a potential blind geothermal system near Battle Mountain, Nevada." *Proceedings: GRC Transactions*, 47, (2023).

Faulds, J.E., Coolbaugh, M.F., Hinz, N.H., Cashman, P.H., and Kratt, C., Dering, G., Edwards, J., Mayhew, B., and McLachlan, H. "Assessment of favorable structural settings of geothermal systems in the Great Basin, western USA." *Proceedings: GRC Transactions*, 35, (2011).

Faulds, J.E., and Hinz, N. "Favorable tectonic and structural settings of geothermal systems in the Great Basin region, western USA: Proxies for discovering blind geothermal systems." *Proceedings, World Geothermal Congress*, (2015).

Faulds, J.E., Hinz, N., Coolbaugh, M., Ayling, B., Glen, J.M.G., Craig, J., McConville, E., Siler, D., Queen, J., Witter, J., and Hardwick, C. "Discovering blind geothermal systems in the Great Basin region: An integrated geologic and geophysical approach for establishing geothermal play fairways. Final technical report for Phases 1-3 (DE-EE0006731)." *Department of Energy*, (2019).

Faulds, J., Earney, T.E., Lindsey, C., Glen, J.M.G., Queen, J.H., Burgess, Q., Giddens, M.H. "Structural Setting and Geothermal Potential of Northeastern Reese River Valley, North-Central Nevada: Highly Prospective Detailed Study Site in the INGENIOUS Project." *Proceedings: GRC Transactions*, 48, (2024) *Same conference*.

Glen, J. M., and Ponce, D. A. "Large-Scale Fractures Related to the Inception of the Yellowstone Hotspot." *Geology*, 30, (2002), doi: 10.1130/0091-7613(2002)030<0647:LSFRTI>2.0.CO;2.

Glen, J.M., and Earney, T.E. "New high resolution airborne geophysical surveys in Nevada and California for geothermal and mineral resource studies." *Proceedings: GRC Transactions*, 48, (2023).

Glen, J.M.G., and Earney, T.E. "GeoDAWN: Airborne magnetic and radiometric surveys of the northwestern Great Basin, Nevada and California." *U.S. Geological Survey Data Release*, (2024), https://doi.org/10.5066/P93LGLVQ.

Grauch, V.J.S., and Cordell, L. "Limitations of determining density or magnetic boundaries from the horizontal gradient of gravity or pseudogravity data." *Geophysics*, (1987), doi: 10.1190/1.1442236.

Hildenbrand, T., Briesacher, A., Flanagan, G., Hinze, W., Hittleman, A., Keller, G., Kucks, R., Plouff, D., Roest, W., Seeley, J., Smith, D., and Webring, M. "Rationale and Operational Plan to Upgrade the U.S. Gravity Database." *U.S. Geological Survey Open File Report*, 02-463, (2002), doi: 10.3133/ofr02463.

Jachens, R.C., and Moring, B.C. "Maps of the Thickness of Cenozoic Deposits and the Isostatic Residual Gravity Over Basement for Nevada." *U.S. Geological Survey Open File Report*, 90-404, (1990), doi: 10.3133/ofr90404.

Jachens, R.C., Moring, B.C., and Schruben P.G. "Thickness of Cenozoic Deposits and the Isostatic Residual Gravity Over Basement" *Chapter 2 in Singer, An Analysis of Nevada's Metal-Bearing Mineral Resources, Nevada Bureau of Mines and Geology Open-File Report*, 96-02-02, (1996).

John, D.A., and Wrucke, C.T. "Geologic map of the Mule Canyon Quadrangle, Lander County, Nevada." *Nevada Bureau of Mines and Geology*, Map 144, (2003).

Kelbert, A., Meqbel, N., Egbert, G.D., Tandon, K. "ModEM: A modular system for inversion of electromagnetic geophysical data." *Computers and Geosciences*, 66, (2014).

McKee, E.H., and Noble, D.C. "Tectonic and magmatic development of the Great Basin of western United States during late Cenozoic time." *Modern Geology*, 10, (1986).

Munoz, G. "Exploring for Geothermal Resources with Electromagnetic Methods." Surveys in *Geophysics*, 35, (2014).

Nevada Bureau of Mines and Geology. "Geothermal Well Information." Accessed from URL https://nbmg.unr.edu/geothermal/WellInfo.html, (accessed, 3/2023a).

Nevada Bureau of Mines and Geology. "Oil and Gas Well Search." Accessed from URL https://nbmg.unr.edu/Oil&Gas/WellSearch.html, (accessed, 3/2023b).

Nevada Division of Water Resources. "Well Driller Reports." Accessed from URL https://data-ndwr.hub.arcgis.com/datasets/NDWR::well-driller-reports/about, (accessed, 3/2023).

Newman, G.A., Gasperikova, E., Hoversten, G.M., Wannamaker, P.E. "Three-dimensional Magnetotelluric Characterization of the Coso Geothermal Field." *Geothermics*, 37, (2008).

Phillips, J.D., Hansen, R.O., and Blakely, R.J. "The use of curvature in potential-field interpretation." *Exploration Geophysics*, 38, (2007).

Ponce, D.A. "Gravity Data of Nevada." *U.S. Geological Survey Data Series*, 42, (1997), doi: 10.3133/ds42.

Ramelli, A.R., House, P.K., Wrucke, C.T., John, D.A. "Geologic map of the Stony Point Quadrangle, Lander County, Nevada." *Nevada Bureau of Mines and Geology*, Map 131, (2001).

Ramelli, A.R., Wrucke, C.T., House, P.K. "Geologic map of the Bateman Spring Quadrangle, Lander County, Nevada." *Nevada Bureau of Mines and Geology*, Map 185, (2017).

Sass, J.H., A.H. Lachenbruch, R.J. Munroe, G.W. Green and T.H. Moses, Jr. "Heat flow in the western United States." *Journal Geophysics Research*, 76, (1971).

Seequent, Oasis Montaj, 2023.2, (2023).

Stewart, J.H., Walker, G.W., and Kleinhampl, F.J. "Oregon-Nevada lineament." *Geology*, 3, (1975).

U.S. Geological Survey: 3D Elevation Program 10-Meter Resolution Digital Elevation Model, accessed from URL https://www.usgs.gov/the-national-map-data-delivery, (accessed, 8/2021a).

U.S. Geological Survey: 3D Elevation Program 1-Meter Resolution Digital Elevation Model, accessed from URL https://www.usgs.gov/the-national-map-data-delivery, (accessed, 8/2021b).

U.S. Geological Survey: Quaternary Fault and Fold Database for the United States, accessed from: https://www.usgs.gov/natural-hazards/earthquake-hazards/faults, (accessed, 7/2021).

Watt, J.T., Glen, J.M.G., John, D.A., Ponce, D.A. “Three-dimensional geologic model of the northern Nevada rift and the Beowawe geothermal system, north-central Nevada.” *Geosphere*, 3, (2007), doi: 10.1130/GES00100.1.

Williams, N., Faulds, J.E., Ayling, B., Glen, J.M.G., Earney, T.E., Siler, D., Kraal, K., Wagoner, N., Morales-Rivera, A. “Analysis of a Blind Geothermal System in the Northern Reese River Basin.” *Proceedings: GRC Transactions*, 46, (2022).

Zeng, Y. “GPS Velocity Field of the Western United States for the 2023 National Seismic Hazard Model Update.” *Seismological Research Letters*, 93, (2022), doi:10.1785/0220220180.

Zoback, M.L., and Thompson, G.A. “Basin and range rifting in northern Nevada: Clues from a mid-Miocene rift and its subsequent offsets.” *Geology*, 6, (1978), doi: 10.1130/00917613(1978)6<111:BARRIN>2.0.CO;2.

Zoback, M.L. “A geologic and geophysical investigation of the Beowawe geothermal area, north-central Nevada.” *Stanford University Publications in the Geological Sciences*, 16, (1979).

Zoback, M.L., McKee, E.H., Blakely, R.J., Thompson, G.A. “The northern Nevada rift: Regional tectono-magmatic relations and middle Miocene stress direction.” *Geological Society of America Bulletin*, 106, (1994).